Conformal curvature flows: from phase transitions to active vision

Satyanad Kichenassamy
Department of Mathematics
University of Minnesota
Minneapolis, MN 55455
email: kichenas@math.umn.edu

Arun Kumar
Department of Aerospace Eng.
University of Minnesota
Minneapolis, MN 55455
email: arun@aem.umn.edu

Peter Olver
Department of Mathematics
University of Minnesota
Minneapolis, MN 55455
email: olver@ima.umn.edu

Allen Tannenbaum
Department of Electrical Engineering
University of Minnesota
Minneapolis, MN 55455
email: tannenba@ee.umn.edu

Anthony Yezzi, Jr.
Department of Electrical Engineering
University of Minnesota
Minneapolis, MN 55455
email: ayezzi@ee.umn.edu

This work was supported in part by grants from the National Science Foundation DMS-8811084, DMS 92-04192, ECS-9122106, by the Air Force Office of Scientific Research F49620-94-1-00S8DEF, by the Army Research Office DAAH04-94-G-0054 and DAAH04-93-G-0332, and by Image Evolutions Limited.

Abstract

In this paper, we analyze geometric active contour models from a curve evolution point of view and propose some modifications based on gradient flows relative to certain new feature-based Riemannian metrics. This leads to a novel edge-detection paradigm in which the feature of interest may be considered to lie at the bottom of a potential well. Thus an edge-seeking curve is attracted very naturally and efficiently to the desired feature. Comparison with the Allen-Cahn model clarifies some of the choices made in these models, and suggests inhomogeneous models which may in return be useful in phase transitions. We also consider some 3-D active surface models based on these ideas. The justification of this model rests on the careful study of the viscosity solutions of evolution equations derived from a level-set approach.

Key words: Active vision, antiphase boundary, visual tracking, edge detection, segmentation, gradient flows, Riemannian metrics, viscosity solutions, geometric heat equations, curve and surface evolution.

This paper has been accepted for publication in **Archive of Rational Mechanics and Analysis.**

1 Introduction

This paper is devoted to the analysis and numerical implementation of the motion of a plane curve in a conformally Euclidean space, and more generally, of surfaces moving by mean curvature, with applications to the detection of contours in an image. The resulting motion presents a much wider range of possible behaviors than the more familiar Euclidean mean curvature flow.

Our motivation comes from the problem of edge-detection in a gray-scale image; however, the equations considered here have a broad range of applications, including phase transitions in particular. In fact, since many edge-detection models implement models arising in other fields (most notably continuum mechanics and statistical mechanics), it seems that it is desirable to develop mathematical tools of universal applicability, which might be useful both within and outside continuum mechanics. Thus, in the present paper, the relation to the Allen-Cahn model illuminates some *ad hoc* choices in image processing, while the introduction of stopping terms in edge-detection suggests inhomogeneous generalizations of the Allen-Cahn model.

1.1 Curvature-related flows in phase transitions

It is well-known that motion by mean curvature arises as one of the possible asymptotic limits in phase field equations. These limiting models include the Allen-Cahn antiphase boundary model [1], the Stefan problem with inclusion of surface tension and kinetic undercooling terms, the Hele-Shaw model, and dendritic solidification; a related problem is thermal grooving (Mullins [51]). The case of more than two phases is addressed by Bronsard & Reitich [14]. A unified derivation of many of the above models can be found in Caginalp [15].

Two typical derivations leading to phase boundaries driven by curvature effects are as follows:

(1) One may start with a parabolic equation of the form

$$u_t = \varepsilon \Delta u + (1/\varepsilon) W'(u),$$

where u is an order parameter, and W is a double-well potential, the minima of which correspond to two phases. The potential is sometimes allowed to depend on ε. As ε tends to zero, it is expected that u tends to either one of these minima, in two regions separated by a sharp interface which moves by its mean curvature. Formal results of this type can be found in Allen & Cahn [1] and Rubinstein, Sternberg & Keller [60], and rigorous justifications in de Mottoni & Schatzman [50], Bronsard & Kohn [13], and Evans, Soner & Souganidis [26]. In this method, the sharp interface is derived as an approximation as the thickness of the region of phase change vanishes. The speed of the interface is the sum of a curvature term and a constant, which we will refer to as the "inflation," see §1.2. The inflation term vanishes if the two minima of W are equal. When present, and negative, it tends to make the interface grow, and can counteract the effect of the curvature term.

(2) One may also directly consider a free-boundary problem, where a function u satisfies the heat equation on both sides of an interface; two boundary conditions are required on the

interface: one relates the speed of the interface to the jump of ∇u in the normal direction, and the other gives u as a combination of the curvature and the speed of the interface. Thus, the interface is not defined by u =const. The effects of the curvature and velocity terms are interpreted, in the context of the Stefan problem, as expressing that the interface includes material in a metastable phase, due to either surface tension effects (curvature) or kinetic undercooling effects (speed).

In both cases, the appearance of the curvature term is clearly due to the Euclidean invariance of the background, and of each of the individual phases. A number of anisotropic models can be found in Gurtin [35, 36] and Angenent & Gurtin [9], together with more references.

1.2 Curvature flow in geometry and image processing

Motion of a curve by its curvature has been extensively studied for its own sake. It is known (Gage [27], Grayson [32, 33], Gage & Hamilton [28]) that a plane curve moving with normal speed equal to its curvature will shrink to a point, its shape becoming smoother and circular. More complicated phenomena are expected in higher dimensions, but no classification is available. This problem can be tackled by the use of the level set method (Osher-Sethian [63, 56]) which consists in viewing the curve as the level set $u = 0$ of a function u constrained to solve the degenerate diffusion equation[1]

$$u_t = \|\nabla u\| \mathrm{div} \frac{\nabla u}{\|\nabla u\|}.$$

Its singular behavior is reflected in the fact that unlike parabolic equations, it is possible to change the solution in the vicinity of one level curve without affecting the rest of the solution. In fact, if the level sets $\{\mathcal{C}(p,t)\}_{p\in\mathbf{R}}$ are well-behaved, this equation is equivalent to the curve evolution

$$\mathcal{C}_t = \kappa \mathcal{N},$$

where $\mathcal{N}$ is the inward normal. However, the PDE formulation allows for singularities to form in this evolution, and provide a way to continue the curve evolution in a unique fashion beyond singularities. Despite its apparent singular form, this equation can be solved in the framework of viscosity solutions (Evans & Spruck [25], Chen, Giga & Goto [18]).

By analogy with fluid mechanics, one may think of the level set formulation as an Eulerian formulation, as opposed to the "Lagrangian" view-point where the motion of points on individual curves is followed.

Curve evolutions can be thought of as describing the motion of a string on the plane; historical remarks and a detailed derivation of the equation for nonlinear vibrating strings can be found in Antman [10]. While these models can be extended to include viscoelastic and other forces, recent work in image processing leads to yet more general curve evolutions. Here, the issue is to find an algorithm which dynamically seeks contours in an image. Kass, Witkin & Terzopoulos (see [39]) have proposed such a procedure whereby a moving contour

[1] Throughout this paper, we use double bars to denote the Euclidean norm.

(a "snake") evolves under the action of intertial, damping, stretching and bending forces, together with an external force which attracts the snake to image-dependent features. The snake model is clearly a generalization of the classical motion of vibrating strings, the modifications being due to the presence of objective features which constrain its evolution. The snake model is sometimes described as that of a rope (with elasticity and rigidity properties) which slides on a landscape to find an equilibrium position.

Translation-invariant curve evolutions, such as the pure curvature evolution, are therefore too restrictive for some applications. We have already seen that the Allen-Cahn equation naturally leads to motions of the type

$$\mathcal{C}_t = (\kappa + \nu)\mathcal{N},$$

with ν constant. However, such a curve evolution would lead, if $\nu < 0$, to a curve growing forever outwards—which is clearly not reasonable: there should be a mechanism to stop the evolution. An *ad hoc* procedure was proposed recently in the context of image processing by Malladi, Sethian & Vemuri [47], and Caselles, Coll, Catté & Dibos [16], for tackling this issue. The problem is to automatically compute outlines in a given gray-level picture, given by its intensity function $I(x, y)$. One can think of it as periodic in x and y. Outlines are by definition regions of high intensity gradient. It is therefore natural to let

$$\phi = \frac{1}{1 + \|\nabla I\|^2},$$

and to expect that a curve evolution given by

$$\mathcal{C}_t = \phi(\kappa + \nu)\mathcal{N},$$

starting outside the desired curve if $\nu > 0$, would tend towards the desired contour. The function ϕ will be referred to as the *stopping term*. Unlike the snake model, this evolution has a level-set ("Eulerian") formulation, and therefore allows contours to form singularities, merge and split (compare with Gupta *et al.* [34]). It is usually convenient to replace I by a smoothed version, using Gaussian smoothing or curvature-based smoothing [61, 62].

1.3 Conformal metrics and curve evolution

We are therefore led to the following conclusions:

(a) Curve evolutions are best studied in a level set ("Eulerian") formulation, which alone allows for the formation of singularities such as breaking and merging;

(b) The pure curvature flow, as well as other homogeneous (translation-invariant) models do not reflect any large-scale inhomogeneities in the background.

We suggest in this paper that curvature evolution in a conformal background is a simple and efficient generalization of Euclidean curve-shortening. Indeed, this amounts to replacing the Laplacian in the Allen-Cahn model by the Laplacian in a conformally Euclidean plane. It would be conceivable to consider more general Riemannian metrics, if the effects of large-scale anisotropies were desired, with little change to the procedures of this paper.

The resulting model is extremely simple:

$$\mathcal{C}_t = \phi(\kappa + \nu)\mathcal{N} - \nabla\phi.$$

The additional gradient term, which was derived from first principles, turns out to provide numerical advantages as well, since it tends to push the moving "snake" towards the desired contour, irrespective of possible overshoots. We do not assume that the conformal factor (ϕ^2) is bounded away from zero. Such a model was also independently proposed in [**?**, **?**].

The two *ad hoc* features of existing models, namely the introduction of the inflation and stopping terms, are clarified by our approach, which also leads us to modify the equation by the addition of a gradient term.

The main difference between our model and pure curvature flow is that the inhomogeneities force the curves to seek special features of the background, instead of shrinking to a point.

Generalized flow by curvature in Riemannian manifolds was also considered by Ilmanen [38], who however does not allow the metric to degenerate. This paper also shows that twice continuoulsy differentiable solutions do not exist in natural situations, thus further illustrating the necessity of viscosity solutions.

Note that proposals advocating the replacement of Euclidean curvature by the affine curvature have been put forward independently by Sapiro & Tannenbaum, and Alvarez, Lions & Morel [3], both in connection with image processing, on an axiomatic basis. Indeed, the affine group is a natural invariance group for plane images, and such an evolution has some advantages in preprocessing (see Sapiro & Tannenbaum [61, 62]). Also, Olver, Sapiro & Tannenbaum [54] have recently recovered this equation from a classification of differential invariants for the affine group. We will however for simplicity consider exclusively the Riemannian curvature only, which we found to give good numerical results.

1.4 Outline of the paper

We now briefly outline the contents of this paper. Section 2 contains some background material on energy-based active contour theory ("snakes"). Section 3 recalls some facts on Euclidean curve shortening. In Sections 4 and 5, we present our modification of the Euclidean arc-length and the resulting active contour models, in two and three dimensions respectively, with brief remarks on what is known for other higher-dimensional surface evolutions. In Section 6, we prove the existence and uniqueness of a continuous solution, Lipschitz in space, for the PDE generated by the level-set approach. Stability with respect to initial conditions is also proved. In addition, by proper choice of initial conditions, one can guarantee that if $\phi = 0$ inside a given contour, a particular level set of u will tend to the set $\phi = 0$. Section 7 analyzes the geodesics of the conformal metric introduced in Sections 4 and 5, and suggests yet another algorithm for edge-detection. Section 8 briefly reports on numerical calculations which illustrate the usefulness of our approach. Finally, in Section 9 we summarize our conclusions.

2 Background on Snakes

In the past few years, a number of approaches have been proposed for the problem of *snakes* or *active contours.* The underlying principle in these works is based upon the utilization of deformable contours which conform to various object shapes and motions. Snakes have been

used for edge and curve detection, segmentation, shape modelling, and visual tracking. The recent book by Blake and Yuille [11] contains an excellent collection of papers on the theory and practice of deformable contours together with a large list of references to which which we refer the interested reader.

In this section, we very briefly sketch the energy based optimization approach to deformable contours as discussed in [39, 71, 11, ?]. Our treatment will of course be very incomplete, and once again we refer the interested reader to [11], especially [72].

In most of the classical frameworks, one considers energy minization methods where controlled continuity splines are allowed to move under the influence of external image dependent forces, internal forces, and certain contraints set by the user. See [39, 71, 11, ?]. As is well-known there may be a number of problems associated with this approach such as initializations, existence of multiple minima, and the selection of the elasticity parameters.

In the present paper, we consider a method which was strongly influenced by the elegant approaches of Caselles *et al.* [16] and Malladi *et al.* [47]. In these works, a level set curve evolution method is presented to solve the problem. Our idea is to note that both these approaches are based on Euclidean curve shortening evolution which in turn defines the gradient direction in which the Euclidean perimeter is shrinking as fast as possible. (See Section 3.) Pushing this concept to the next logical step, we can derive new active contour models by multiplying the Euclidean arc-length by a function tailored to the features of interest to which we want to flow, and then writing down the resulting *gradient evolution equations.* Mathematically, this amounts to defining a new Riemannian metric in the plane tailored to the given image, and then computing the corresponding gradient flow. This leads to some new snake models which efficiently attract the given active contour to the features of interest (which basically lie at the bottom of a *potential well*). The method also allows us to naturally write down 3-D active surface models as well. One can completely justify this method using the method of viscosity solutions. A preliminary version of these results has been reported in [40].

Let $C(p) = (x(p), y(p))^T$ be a closed contour in R^2 where $0 \leq p \leq 1$. (Note that the superscript T denotes transpose.) We now define an energy functional on the set of such contours ("snakes"), $\mathcal{E}(C)$. Following standard practice, we take $\mathcal{E}(C)$ to be of the form

$$\mathcal{E}(C) = \mathcal{E}_{int}(C) + \mathcal{P}(C),$$

where $\mathcal{E}_{int}$ is the *internal deformation energy* and $\mathcal{P}$ is an external potential energy which depends on the image. (Other external constraint forces may be added.) A common choice for the internal energy is the quadratic functional

$$\mathcal{E}_{int}(C) := \int_0^1 w_1(p)\|C_p\|^2 + w_2(p)\|C_{pp}\|^2 dp,$$

where w_1 and w_2 control the "tension" and "rigidity" of the snake, respectively. (Note that the subscripts denote derivatives with respect to p in the latter expression, and $\|\cdot\|$ denotes the standard Euclidean norm.)

Let $I : R^2 \to R$ be the given grey-scale image. Then the external potential energy depends on the image $I(x, y)$. It can be defined by

$$\mathcal{P}(C) := \int_0^1 P(C(p))dp,$$

where $P(x,y)$ is a scalar potential function defined on the image plane. The local minima of P attract the snake. For example, we may choose P to be

$$P(x,y) := c\|\nabla G_\sigma * I(x,y)\|,$$

for a suitably chosen constant c, in which case the snake will be attracted to intensity edges. Here G_σ denotes a Gaussian smoothing filter of standard deviation σ.

One also typically considers dynamic time-varying models in which $C(p)$ becomes a function of time as well; see [72]. In this case, one defines a kinetic energy and the corresponding Lagrangian (the difference between the kinetic energy and the energy $\mathcal{E}$ defined above). Applying the principle of least action, one derives the corresponding Lagrange equation which one tries to solve numerically employing various approximations.

In the approach to be given below in Section 4, we will also use an energy method. However, in contrast to more *ad hoc* approaches, we believe that our energy is intrinsic to the given geometry of the problem, as is the correspondent gradient flow.

3 Curve Shortening Flows

The motivation for the equations underlying active geometric contours comes from *Euclidean curve shortening.* Therefore, in this section we will review the relevant curve evolution theory in the plane R^2.

Accordingly, for κ the curvature, and $\vec{\mathcal{N}}$ the inward unit normal, one considers families of plane curves evolving according to the *geometric heat equation*

$$\frac{\partial C}{\partial t} = \kappa\vec{\mathcal{N}}. \tag{1}$$

This equation has a number of properties which make it very useful in image processing, and in particular, the basis of a nonlinear scale-space for shape representation [2, 4, 41, 42, 48].

Indeed, (1) is the Euclidean curve shortening flow, in the sense that the Euclidean perimeter shrinks as quickly as possible when the curve evolves according to (1) [27, 28, 32]. Since, we will need a similar argument for the snake model we discuss in the next section, let us work out the details.

Let $C = C(p,t)$ be a smooth family of closed curves where t parametrizes the family and p the given curve, say $0 \le p \le 1$. (Note we assume that $C(0,t) = C(1,t)$ and similarly for the first derivatives with respect to p.) Consider the length functional

$$L(t) := \int_0^1 \|\frac{\partial C}{\partial p}\|dp.$$

Then differentiating (taking the "first variation"), and using integration by parts, we see that

$$\begin{aligned} L'(t) &= \int_0^1 \frac{\langle \frac{\partial C}{\partial p}, \frac{\partial^2 C}{\partial p \partial t}\rangle}{\|\frac{\partial C}{\partial p}\|}dp \\ &= -\int_0^1 \langle \frac{\partial C}{\partial t}, \frac{1}{\|\frac{\partial C}{\partial p}\|}\frac{\partial}{\partial p}\left[\frac{\frac{\partial C}{\partial p}}{\|\frac{\partial C}{\partial p}\|}\right]\|\frac{\partial C}{\partial p}\|\rangle dp. \end{aligned}$$

(Note that we multiplied and divided by $\|\frac{\partial C}{\partial p}\|$ in the latter integral.) But observing now that

$$\|\frac{\partial C}{\partial p}\|dp =: ds$$

is (Euclidean) arc-length, and using the standard definition of curvature, the last integral is

$$-\int_0^{L(t)} \langle \frac{\partial C}{\partial t}, \kappa \vec{\mathcal{N}} \rangle ds.$$

That is, we see

$$L'(t) = -\int_0^{L(t)} \langle \frac{\partial C}{\partial t}, \kappa \vec{\mathcal{N}} \rangle ds.$$

Thus the direction in which $L(t)$ is decreasing most rapidly is when

$$\frac{\partial C}{\partial t} = \kappa \vec{\mathcal{N}}.$$

Thus (1) is precisely a gradient flow.

A much deeper fact is that simple closed curves converge to "round" points when evolving according to (1) without developing singularities; see [28, 32]. This fact is one of the keys for the geometric active contour models considered below.

4 2D Active Contour Models

In two elegant papers, Caselles *et al.* [16] and Malladi *et al.* [47] propose a snake model based on the level set formulation of the Euclidean curve shortening equation. More precisely, their model is

$$\frac{\partial \Psi}{\partial t} = \phi(x,y)\, \|\nabla \Psi\| \left(\mathrm{div} \left[\frac{\nabla \Psi}{\|\nabla \Psi\|} \right] + \nu \right). \tag{2}$$

Here the function $\phi(x,y)$ depends on the given image and is used as a "stopping term." For example, the term $\phi(x,y)$ may chosen to be small near an edge, and so acts to stop the evolution when the contour gets close to an edge. In [16, 47], the term

$$\phi := \frac{1}{1 + \|\nabla G_\sigma * I\|^n} \tag{3}$$

is chosen, where I is the (grey-scale) image and G_σ is a Gaussian (smoothing) filter. (In [16], $n = 1$, and in [47], $n = 2$.) The function $\Psi(x,y,t)$ evolves in (2) according to the associated level set flow for planar curve evolution in the normal direction with speed a function of curvature which was introduced in the fundamental work of Osher-Sethian [55, 56, 63, 64, 65].

It is important to note that as we have seen above, the Euclidean curve shortening part of this evolution, namely

$$\frac{\partial \Psi}{\partial t} = \|\nabla \Psi\| \mathrm{div} \left[\frac{\nabla \Psi}{\|\nabla \Psi\|} \right] \tag{4}$$

is derived as a gradient flow for shrinking the perimeter as quickly as possible. As is explained in [16], the constant *inflation term* ν is added in (2) in order to keep the evolution moving in the proper direction.

Remarks 1.

1. In [47], the inflationary constant ν is considered both with a positive sign (inward evolution of the contour in the direction of decreasing Ψ) and with a negative sign (outward or expanding evolution). (Usually, Ψ is taken to be smaller inside a level set contour, e.g., it is negative in the interior and positive in the exterior of the zero level set.) In the latter case, this can be referred to as expanding "balloons" [**?**]. For simplicity, unless stated otherwise explicitly, we will take $\nu \geq 0$ (inward evolutions) in what follows below.

2. Instead of using a Gaussian to smooth the image one may of course use a nonlinear smoothing filter based on the curvature; see [5].

3. There are of course many possibilities for a stopping term besides intensity: texture, optical flow, stereo disparity, etc.

We would like to modify the model (2) in a manner suggested by the computation in Section 3. Namely, we will change the ordinary Euclidean arc-length function along a curve $C = (x(p), y(p))^T$ with parameter p given by

$$ds = \|C_p\|\, dp = \sqrt{x_p^2 + y_p^2}\, dp$$

to

$$ds_\phi = \phi\, ds = \phi(x, y)\sqrt{x_p^2 + y_p^2}\, dp,$$

where $\phi(x, y)$ is a positive differentiable function. We now essentially repeat the computation made in Section 3, i.e., we want to compute the corresponding gradient flow for shortening length relative to the new metric ds_ϕ.

Accordingly set

$$L_\phi(t) := \int_0^1 \|\frac{\partial C}{\partial p}\|\phi\, dp.$$

Let

$$\vec{\mathcal{T}} := \frac{\partial C}{\partial p}/\|\frac{\partial C}{\partial p}\|,$$

denote the unit tangent. Then taking the first variation of the modified length function L_ϕ, and using integration by parts just as above, we get that

$$-L'_\phi(t) \;=\; \int_0^{L_\phi(t)} \langle \frac{\partial C}{\partial t}, \phi\kappa\vec{\mathcal{N}} + (\nabla\phi \cdot \vec{\mathcal{T}})\vec{\mathcal{T}} - \nabla\phi\rangle ds$$

which means that the direction in which the L_ϕ perimeter is shrinking as fast as possible is given by

$$\frac{\partial C}{\partial t} = \phi\kappa\vec{\mathcal{N}} + (\nabla\phi \cdot \vec{\mathcal{T}})\vec{\mathcal{T}} - \nabla\phi. \tag{5}$$

This is precisely the gradient flow corresponding to the miminization of the length functional L_ϕ. Since the tangential component of equation (5) may be dropped (see [24]), this may be simplified to

$$\frac{\partial C}{\partial t} = \phi \kappa \vec{\mathcal{N}} - \nabla \phi. \tag{6}$$

The level set version of this is

$$\frac{\partial \Psi}{\partial t} = \phi \, \|\nabla \Psi\| \mathrm{div} \left[\frac{\nabla \Psi}{\|\nabla \Psi\|} \right] + \nabla \phi \cdot \nabla \Psi. \tag{7}$$

One expects that this evolution should attract the contour very quickly to the feature which lies at the bottom of the *potential well* described by the gradient flow (7). As in [16, 47], we we may also add a constant inflation term (which may be interpreted as a Lagrange multiplier for a constrained version of the given optimization problem), and so derive a modified model of (2) given by

$$\frac{\partial \Psi}{\partial t} = \phi \, \|\nabla \Psi\| \left(\mathrm{div} \left[\frac{\nabla \Psi}{\|\nabla \Psi\|} \right] + \nu \right) + \nabla \phi \cdot \nabla \Psi. \tag{8}$$

Notice that for ϕ as in (3), $\nabla \phi$ will look like a doublet near an edge. Of course, one may choose other candidates for ϕ in order to pick out other features.

We have implemented this snake model based on the algorithms of Osher-Sethian [55, 56, 63, 64, 65] and Malladi *et al.* [47]. We are also experimenting with some new code based on [53]. Some preliminary numerical results based on our code will be presented in Section 8 below.

Remarks 2.

Note that the metric ds_ϕ has the property that it becomes small where ϕ is small and vice versa. Thus at such points lengths decrease and so one needs less "energy" in order to move. Consequently, it seems that such a metric is natural for attracting the deformable contour to an edge when ϕ has the form (3).

5 3-D Active Contour Models

In this section, we will discuss some possible geometric 3-D contour models based on surface evolution ideas, by modifying the Euclidean area in this case by a function which depends on the salient features which we wish to capture. In order to do this, we will need to set up some notation. (For all the relevant concepts on the differential geometry of surfaces, we refer the reader to [22].) We remark that all of these considerations can be straightforwardly extended to the evolution of hypersurfaces in n-dimensional space.

Let $S : [0,1] \times [0,1] \to R^3$ denote a compact embedded surface with (local) coordinates (u, v). Let H denote the mean curvature and $\vec{\mathcal{N}}$ the inward unit normal. We set

$$S_u := \frac{\partial S}{\partial u}, \quad S_v := \frac{\partial S}{\partial v}.$$

Then the infinitesimal area on S is given by

$$dS = \sqrt{\|S_u\|^2\|S_v\|^2 - \langle S_u, S_v\rangle^2}\, du\, dv.$$

Let $\phi : \Omega \to R$ be a positive differentiable function defined on some open subset of R^3. The function $\phi(x, y, z)$ will play the role of the "stopping" function ϕ given above in our snake model (7, 8).

It is a beautiful classical fact that the gradient flow associated to the area functional for surfaces (i.e., the direction in which area is shrinking most rapidly) is given by

$$\frac{\partial S}{\partial t} = H\vec{\mathcal{N}}. \tag{9}$$

(See [12, 30, 49, 54, 73] and the references therein.) What we propose to do is to replace the Euclidean area by a modified area depending on ϕ namely,

$$dS_\phi := \phi\, dS.$$

For a family of surfaces (with parameter t), consider the ϕ-area functional

$$A_\phi(t) := \int\int_S dS_\phi.$$

Once again, an integration by parts argument gives that

$$\frac{dA_\phi}{dt} = -\int\int_S \langle \frac{\partial S}{\partial t}, \phi H\vec{\mathcal{N}} - \nabla\phi + \text{tangential components}\rangle\, dS,$$

which after dropping the tangential part becomes

$$\frac{\partial S}{\partial t} = \phi H\vec{\mathcal{N}} - \nabla\phi. \tag{10}$$

The level set version of (10) is given in terms of $\Psi(x, y, z, t)$ by

$$\Psi_t = \phi\ \|\nabla\Psi\|\text{div}\left[\frac{\nabla\Psi}{\|\nabla\Psi\|}\right] + \nabla\phi\cdot\nabla\Psi. \tag{11}$$

As before one may add a constant inflation term to the mean curvature to derive the model

$$\Psi_t = \phi\|\nabla\Psi\|\left(\text{div}\left[\frac{\nabla\Psi}{\|\nabla\Psi\|}\right] + \nu\right) + \nabla\phi\cdot\nabla\Psi. \tag{12}$$

In the context of image processing, the term ϕ depends on the given 3-D image and is exactly analogous to the stopping term in (7, 8). It is important to note that there is a very big difference between the 2-D and 3-D models discussed here. Indeed, the geometric heat equation will shrink a simple closed curve to a round point without developing singularities, even if the initial curve is *nonconvex*. The geometric model (2) is based on this flow. For surfaces, it is well-known that singularities may develop in the mean curvature flow (9) non-convex smooth surfaces [31]. (The classical example is the dumbbell.) We should note

however that the mean curvature flow does indeed shrink smooth compact convex surfaces to round "spherical" points; see [37].

We should add that because of these problems, several researchers have proposed replacing mean curvature flow by flows which depend on the Gaussian curvature κ. Indeed, define

$$\kappa_+ := \max\{\kappa, 0\}.$$

Then Caselles and Sbert [17] have shown that the *affine invariant flow*

$$\frac{\partial S}{\partial t} = \text{sign}(H)\kappa_+^{1/4}\vec{\mathcal{N}} \tag{13}$$

will (smoothly) shrink rotationally symmetric compact surfaces to ellipsoidal shaped points. (This has been proven in [7] in the convex case. See also [3, 6].) Thus one could replace the mean curvature part by $\text{sign}(H)\kappa_+^{1/4}$ in (12). Another possibility would be to use $\kappa_+^{1/2}$ as has been proposed in [52]. See also [70]. (Note that Chow [19] has shown that convex surfaces flowing under $\kappa^{1/2}$ shrink to spherical points.) All these possible evolutions for 3-D contours are now being explored. See also Section 7 below for a possible alternative related approach to 3D segmentation.

6 Viscosity Analysis of the Models

In this section, we will outline the analysis of the nonlinear diffusion equation

$$\Psi_t = \phi(x)a^{ij}(\nabla\Psi)\partial_{ij}\Psi + H(x, \nabla\Psi), \quad x = (x_1, \ldots, x_n), \tag{14}$$

of which the models of Caselles *et al.* [16] and Malladi *et al.* [47], and the equations we study here are special cases. Note that we use the summation convention systematically in (14) and in what follows. This section is rather mathematically technical, and has been included to rigorously justify the partial differential equations we have been using. We use the standard notation from the theory of partial differential equations as may be found in [67].

Because of the form of a^{ij}, and the fact that ϕ may vanish, this problem requires some care; in particular, the solutions are not expected to be sufficiently regular for the equation to make sense, and we need to use a type of generalized solutions known as *viscosity solutions*, defined below. The technicalities are very similar to those in [4], [16].

In what follows, the letter C is used to denote various positive constants, the exact value of which is not significant. We assume that H is the sum of $\nabla\Psi \cdot \nabla\phi$ and an "inflation term" $\nu\phi\|\nabla\Psi\|$. We also assume that ϕ and $\sqrt{\phi}$ are Lipschitz continuous. While ϕ and H are continuous in their arguments, a^{ij} is not:

$$a^{ij}(p) = \delta^{ij} - \frac{p_i p_j}{\|p\|^2}, \quad p = (p_1, \ldots, p_n),$$

where δ^{ij} denotes the Kronecker delta. We use periodic boundary conditions in the spatial domain, and consider a Lipschitz continuous initial value $\Psi_0(x)$. Our solutions will have bounded first derivatives, but will not have second-order derivatives in general.

Viscosity interpretation of equation (14):

Since the solution is not twice differentiable, we must use a notion of *weak solution.* Since the equation is not in the form of a divergence, the familiar integration by parts argument used for shock waves does not help.

Therefore, we are led to use the notion of "viscosity solution," which has proved useful in this context.

We first define sub- and super-solutions of equation (14). Let $T > 0$. A function f is said to be a *sub-solution* if f is defined and continuous for all x, and $0 \leq t \leq T$ for some $T > 0$, and is such that whenever g is a twice continuously differentiable function and $(f - g)$ attains a local maximum at a point (x_0, t_0) with $t_0 > 0$, one has

$$g_t(x_0, t_0) - \phi(x_0) a^{ij}(Dg(x_0, t_0))\partial_{ij} g(x_0, t_0) - H(x_0, \nabla g(x_0, t_0)) \leq 0,$$

if $\nabla g(x_0, t_0) \neq 0$. If $\nabla g(x_0, t_0) = 0$, we require instead

$$g_t(x_0, t_0) - \phi(x_0) \limsup_{p \to 0} a^{ij}(p)\partial_{ij} g(x_0, t_0) - H(x_0, \nabla g(x_0, t_0)) \leq 0;$$

this latter form being made necessary by the fact the a^{ij} is not continuous for $p = 0$. A *super-solution* is similarly defined, by requiring that $(f - g)$ have a local minimum, replacing lim sup by lim inf, and reversing the direction of all inequalities. A *viscosity solution* is, by definition, a continuous function which is both a sub- and a super-solution.

We can now state the following result:

Theorem 1 *There is a unique viscosity solution in* $L^\infty(0, T; W^{1,\infty}(R^n))$.

Proof. The construction of the solution proceeds by solving an approximate uniformly parabolic problem, and by passing to the limit. The uniqueness is more delicate and requires a lemma from Crandall-Ishii [20]; the outcome will be an estimate for the difference of two solutions with different initial data.

STEP 1: (Gradient bounds).
We consider here the case when the nonlinearities are all smooth. These considerations will apply to a regularized version of our equation. In the following, subscripts denote derivatives.

Let Ψ be a solution. Differentiation of the equation gives

$$\partial_t \Psi_k - \phi_k a^{ij} \Psi_{ij} - \phi \left[\frac{\partial a_{ij}}{\partial p^l} \Psi_{lk} \Psi_{ij} + a^{ij} \Psi_{ijk} \right] - \frac{\partial H}{\partial p_l} \Psi_{lk} - \frac{\partial H}{\partial x^k} = 0.$$

We multiply this equation by $2\Psi_k$ and sum over k to find:

$$M_t - \phi \left[a^{ij} \partial_{ij} M + \frac{\partial a_{ij}}{\partial p^l} \Psi_{ij} \partial_l M \right] + \frac{\partial H}{\partial p_l} M_l = -2\phi a^{ij} \Psi_{ik} \Psi_{jk} + 2\partial_k \phi \left[a^{ij} \Psi_{ij} \Psi_k + H \Psi_k \right],$$

where $M = \|\nabla \Psi\|^2$.

We now choose our approximation: we replace a^{ij} and ϕ by

$$a^{ij}_\varepsilon = \varepsilon \delta^{ij} + \left(\delta^{ij} - \frac{p_i p_j}{\|p\|^2 + \varepsilon^2} \right); \quad \phi_\varepsilon = \phi + \varepsilon.$$

We also replace $\|\nabla\Psi\|$ by $\sqrt{\|\nabla\Psi\|^2+\varepsilon^2}$ in the inflation term.

Since we assumed that $\sqrt{\phi}$ is Lipschitz, we have

$$|\partial_k\phi_\varepsilon| \le C\sqrt{\phi} \le C\sqrt{\phi_\varepsilon}.$$

On the other hand, reducing the symmetric semi-definite matrix (a^{ij}) to its principal axes, it is easy to see that

$$(a^{ij}\Psi_{ij})^2 \le C(a^{ij}\Psi_{ik}\Psi_{jk})$$

for some constant C. Combining these two estimates, and using $H \le C\|\nabla\Psi\|$, we find, using the maximum principle for uniformly parabolic equations, that

$$\|\nabla\Psi\|_{L^\infty}(t) \le e^{Ct}(\|\nabla\Psi\|_{L^\infty}(0)+\varepsilon^2).$$

A global Lipschitz estimate in space for solutions of the approximate equation follows.

STEP 2: (Convergence of approximations).
The gradient bound in space implies in fact a Hölder estimate with exponent $1/2$ in time. We may therefore apply Ascoli's theorem to conclude that a solution exists. To prove its uniqueness will require more sophisticated tools from the theory of viscosity solutions.

STEP 3: (Comparison principle and uniqueness).
Let two solutions Ψ_1 and Ψ_2 be given (both in the viscosity sense). We define

$$\alpha(x,y,t) = \Psi_1(t,x) - \Psi_2(y,t) - (4\varepsilon)^{-1}\|x-y\|^4 - \lambda t,$$

where λ is an arbitrary positive constant. We claim that on $0 \le t \le T$, this function is maximum for $t = 0$. Indeed, otherwise, the maximum would be attained at some point (x_0, y_0, t_0) with $t_0 > 0$. By a lemma of Crandall and Ishii [20], for any positive μ, there are real numbers a and b, and symmetric matrices X and Y such that

$$a - b = \lambda$$

and

$$\begin{pmatrix} X & 0 \\ 0 & -Y \end{pmatrix} \le A + \mu A^2,$$

where

$$A = \begin{pmatrix} B & -B \\ -B & B \end{pmatrix},$$

with

$$B_{ij} = \varepsilon^{-1}\|x_0-y_0\|^2\delta_{ij} + (2/\varepsilon)(x_0-y_0)_i(x_0-y_0)_j.$$

In addition, one has

$$a - \phi(x_0)a^{ij}(\varepsilon^{-1}\|x_0-y_0\|^2(x_0-y_0))X_{ij} - H(\varepsilon^{-1}\|x_0-y_0\|^2(x_0-y_0)) \le 0$$

and

$$b - \phi(y_0)a^{ij}(\varepsilon^{-1}\|x_0 - y_0\|^2(x_0 - y_0))Y_{ij} - H(y_0, \varepsilon^{-1}\|x_0 - y_0\|^2(x_0 - y_0)) \geq 0.$$

If $x_0 = y_0$, these relations have to be interpreted in terms of a suitable limit, but this case leads to $a \leq 0 \leq b$, which contradicts the assumption $\lambda > 0$. So $x_0 \neq y_0$.

Next, choose $\mu = \varepsilon\|x_0 - y_0\|^{-2}$ (which is now possible), and conclude that

$$\begin{pmatrix} X & 0 \\ 0 & -Y \end{pmatrix} \leq \frac{2}{\varepsilon}\begin{pmatrix} D & -D \\ -D & D \end{pmatrix},$$

where

$$D_{ij} = \|x_0 - y_0\|^2\delta_{ij} + 5(x_0 - y_0)_i(x_0 - y_0)_j.$$

Multiplying this inequality by G, where

$$G = \begin{pmatrix} \phi(x_0)B & \sqrt{\phi(x_0)\phi(y_0)}B \\ \sqrt{\phi(x_0)\phi(y_0)}B & \phi(y_0)B \end{pmatrix},$$

and taking the trace, we obtain after some manipulation, using the fact that a^{ij} is bounded, the definition of a viscosity solution, and the fact that $\sqrt{\phi}$ is Lipschitz, an inequality

$$\lambda \leq C_0\|x_0 - y_0\|^4/\varepsilon.$$

Using the Lipschitz condition on the functions Ψ_1 and Ψ_2, and the property $\alpha(t_0, x_0, y_0) \geq \alpha(t_0, y_0, y_0)$, we derive a bound

$$\lambda \leq C\varepsilon^{1/3}L^{4/3}.$$

Taking

$$\varepsilon^{1/3} = \delta K$$

and

$$\lambda = 2C_0\delta K L^{4/3},$$

with $K = \sup_{[0,T]\times R^n}|\Psi_1 - \Psi_2|$, we find that the bound on λ leads to an absurdity. We therefore can conclude that $t_0 = 0$.

We fix λ and ε as before. Using $t_0 = 0$, we find that

$$\sup_{[0,T]\times R^n}|\Psi_1 - \Psi_2| \leq \sup_{R^n}|\Psi_1 - \Psi_2|(0) + \frac{3}{4}\delta K L^{4/3} + 2C_0\delta K L^{4/3}T.$$

Letting $\delta \to 0$, we finally obtain

$$\sup_{[0,T]\times R^n}|\Psi_1 - \Psi_2| \leq \sup_{R^n}|\Psi_1 - \Psi_2|(0),$$

which proves uniqueness and stability with respect to initial conditions. □

We can conclude from Theorem 1 that slight differences between images will not become artificially enhanced by our active contour methods.

Convergence of level sets:

The next task is to show that the level curves of the function Ψ do approach the desired contour $\Gamma = \{\phi = 0\}$. To prove this, we construct a subsolution which is initially no greater than the solution, and which becomes eventually positive at any point outside the contour. We give the argument in two space dimensions for convex contours, it being understood that smooth non-convex contours can be handled as in [16]. It will be clear that the addition of the gradient term enables one to relax the size conditions on the inflation parameter.

We consider, to simplify, the case of a contour Γ which will be taken to be included in the unit square $[0,1]^2$ to fix ideas. We assume that Γ is smooth and separates the square into two regions, the inside $I(\Gamma)$ and the outside $E(\Gamma)$. Furthermore, ϕ vanishes identically on the contour, and the distance function $d(x) = d(x,\Gamma)$ is smooth on $E(\Gamma)$ (one can get around this requirement if the region between Γ and the boundary of the square can be mapped to an annulus, in the spirit of [16]). To make calculations more explicit, we simply take $\phi = \phi(d(x))$ to be an increasing function of the distance to Γ in $E(\Gamma)$.

We also assume that the initial value of Ψ is itself a nonnegative subsolution (independent of time) vanishing on the contour Γ.

Remark 3.

To find such an initial value, it suffices to take Ψ_0 to be a smooth function of the distance to Γ, vanishing for $d = 0$, and equal to 1 for large d, and then to take ν large enough. This is rather similar to the initialization one would take for the numerical computation itself.

Theorem 2 *Let $\eta > 0$. There is, if ν is large enough, a subsolution $w(x,t)$ on $E(\Gamma)$ which satisfies $w(x,0) \leq \Psi_0(x)$ and such that for every x with $d(x) > \eta$, $w(x,t) > 0$ for t large enough.*

By applying the comparison principle on $E(\Gamma)$, we conclude that the level set $\Psi = 0$ must tend towards Γ, as desired.

Proof. We proceed in four steps.

STEP 1: (Definition of w).
We let

$$w(x,t) = \lambda f(t) k(d(x)) + g(t)$$

where λ is a positive number, f, g and k are smooth in their arguments, and satisfy

1. $f(0) = g(0) = k(0) = 0$, $g'(t) \leq 0$, $k' \geq 0$.
2. There is a number t_1 such that f is increasing, f' is decerasing, and $g' \leq \alpha < 0$ for $t \leq t_1$.
3. For $t \geq t_1$, $f' \leq 0$ and $g' \leq 0$.

4. $\lim_{t\to\infty} f(t) = 1$, $\lim_{t\to\infty} g(t) = 2\alpha t_1$.

Note that by choosing k suitably, one can give any required smoothness to the function obtained by extending w by zero in $I(\Gamma)$. α and λ are chosen below.

STEP 2: (w is a subsolution).
Substituting into the equation, we find that we need

$$\lambda f'(t)k(d) + g'(t) - \lambda f k'[\phi(d)(\Delta d + \nu) + \phi'(d)] \leq 0.$$

Let us require that

$$\phi(d)(\Delta d + \nu) + \phi'(d) \geq 0.$$

This can certainly be achieved by taking ν large. Note that without the gradient term, we would have been led to $\Delta d + \nu \geq 0$. Then, for $t \geq t_1$, we find that all terms are nonpositive, whereas for $t \leq t_1$, the first and third terms are nonincreasing in t, while $g' \leq \alpha$. It therefore suffices to have

$$\lambda f'(0)k(d) + \alpha \leq 0.$$

STEP 3: ($w \leq u$).
We want to show that $w \leq u$ on the boundary of $E(\Gamma)$ for all time, as well as initially on all of $E(\Gamma)$. For $t = 0$, $w = 0$. On Γ, $w = g$, which is non-positive. As for the outer boundary, it suffices to show that $w \leq \Psi_0$, since Ψ_0 is a subsolution (so that $\Psi_0 \leq \Psi$). Now, on the outer boundary of $E(\Gamma)$, we know that Ψ_0 is positive, so we merely need to ensure w is small. This can be ensured by making λ small.

STEP 4: (w is eventually positive).
For fixed x, we see that

$$\lim_{t\to\infty} w(t) = \lambda k(d(x)) + 2\alpha t_1.$$

Therefore, if $\alpha > -\lambda k(\eta)/2$, we are guaranteed that w is eventually positive.

This completes the proof of Theorem 2. □

We can now conclude that the solution Ψ will become eventually positive outside Γ so that its zero level set must approach the desired contour. We have therefore shown that the model of the present paper is justified from a theoretical standpoint. Further practical consequences of the discussion in this section are:

(1) If ϕ is not rigorously zero on the desired contour, the evolution has no reason to stop. In fact, one would rather expect it to shrink the snake to a point. This explains why in dealing with poor images, one may see the snake passing through the features of interest. This is a further advantage of an additional stopping term. Some care must therefore be given to the choice of ϕ, so that the evolution slows down significantly near the desired contour.

(2) The appropriate amount of inflation can be estimated (from above) from the construction of our subsolution. Without the gradient term, it is safe to take an inflation term of the order of the curvature of the desired contour.

7 Geodesic Paths

Given that we are now looking at a Riemannian metric, it becomes natural to investigate its geodesics. It turns out that the geodesics appear to have a very concrete interpretation in this problem. For background on the problem of finding closed geodesics on manifolds in connection with curve-shortening, see [23, 28, 32, 33].

The geodesics of the conformally Euclidian metric considered in this paper are solutions to an *ordinary differential equation* which can be used both for the segmentation and edge detection problem. For simplicity, we work in the plane once again with the stopping function ϕ as discussed in Section 4. As before we modify the Euclidean metric by taking $ds_\phi = \phi ds$. Indeed, setting $u = \phi^2$, we find that the equation of geodesics takes the form [23]

$$C_{pp} + \frac{\langle C_p, \nabla u \rangle C_p - \frac{1}{2}\|C_p\|^2 \nabla u}{u} = 0. \tag{15}$$

Note that the tangential term $(C_p, \nabla u)C_p$ can be removed by change of parametrization.

Define the "potential function"

$$V(C) = E - \frac{\phi^2}{2},$$

where E is a certain constant which we describe below. Given this we claim that solutions of the oscillator-type equation

$$C_{qq} + \nabla V(C) = 0 \tag{16}$$

can be reparametrized to give geodesics of the line element ds_ϕ where This may be seen from the following calculation. Start with the equation (15). Since we have the first integral

$$\frac{1}{2}\|C_q\|^2 + V(C) = E,$$

equation (16) can be written as

$$C_{qq} + \frac{\|C_q\|^2}{2(E - V)}\nabla V = 0, \tag{17}$$

which is precisely (15) up to tangential term.

In terms of the image, what we want is to locate a potential valley. Therefore, an algorithm using geodesics might be as follows: run a geodesic with zero initial speed, and stop when its velocity starts to decrease. This should approximately give a point on the desired contour. Of course, one may want to add a stopping term too. Also, such a geodesic, if launched in the correct direction, should tend to *go around* the desired object—this might be useful to get an initial guess, and for segmentation.

We should note that the above computation remains valid in any number of space dimensions. For surfaces, these curves would swirl about the desired object. Since the equations are conservative, we are guaranteed that the curves will not wander too far away. Numerical calculations using this idea will be reported elsewhere.

8 Numerical Calculations

We will now give a few numerical calculations to illustrate our methods. The implementations we have used are based on the level set evolution methods developed by Osher-Sethian [55, 56, 63, 64, 65], and the techniques in [47]. The equations described in this paper have been coded for the case of active contours on two-dimensional images. The code is still in an early form and work is in progress to improve various aspects of it. We will present here some preliminary experimental results obtained by running this code on both binary (i.e., high contrast images) and real images. At this stage of the work the images have been selected purely for the purposes of illustration. The images are sampled at discrete pixel locations as usual.

8.1 Numerical Aspects of Level Set Evolution

For 2D active contours, the evolution equation as derived in Section 4 is equation (8),

$$\frac{\partial \Psi}{\partial t} = \phi \|\nabla \Psi\| \left(\mathrm{div} \left[\frac{\nabla \Psi}{\|\nabla \Psi\|} \right] + \nu \right) + \nabla \phi \cdot \nabla \Psi,$$

where ν is a constant inflation force and $\kappa := \mathrm{div}(\frac{\nabla \Psi}{\|\nabla \Psi\|})$ is the curvature of the level sets of $\Psi(x, y, t)$. This equation describes a propagating front, and we are interested in its propagation in the plane of an image. It is known that a propagating front may not remain smooth at all times (for example, it may cross itself). For evolution beyond the discontinuities the solutions are required to satisfy an entropy condition to ensure that the front remains physically meaningful at all times. The discrete approximations to the spatial derivatives are thus derived from the entropy condition. Osher-Sethian [56] have given such entropy satisfying schemes and these have been used successfully in shape modelling [47]. Following [47] we can regard a decomposition of our speed function as,

$$F(\kappa) = \nu + \mathrm{div}(\frac{\nabla \Psi}{\|\nabla \Psi\|}) = \nu + \kappa, \tag{18}$$

where ν is regarded as the constant passive advection term and the curvature κ is the diffusive term of the speed function. The inflation part in equation (8), i.e., $\nu\phi\|\nabla\Psi\|$ is approximated using upwind schemes. The diffusive part, i.e., $\kappa\phi\|\nabla\Psi\|$ is approximated using the usual central differences. For the inner product term $\nabla\phi \cdot \nabla\Psi$, we use a certain thresholding smoothing method for the "doublet" $\nabla\phi$ which will be described in full detail in another paper.

As discussed in [47], an important aspect of the propagation as given in equation (8) is that the image-based terms only have meaning on the zero-level set. Thus these terms must be extended to all the level sets to get a globally defined *extension*. To do this, we have basically followed the methods reported in [47] to which we refer the reader for all the details.

There are also stability implications of the choice of the step sizes, and in [47] it is noted that for the evolution equation used in that work the requirement is $\Delta t = O(\Delta x^2)$. Therefore if small spatial step sizes are used, it forces a small time step and the resulting evolution

can be very slow. One way to speed up the evolution is to use a larger inflationary force and move the front faster (recall the advection term causes a constant contraction/expansion of the front). However, in our experience with using the approach in [47] this results in large motion of the front causing "overshooting" of the edge of the feature of interest in the image, because ϕ might not be rigorously zero on the desired contour. This problem is resolved by the evolution in equation (8). The gradient term $\nabla\phi$ has a behavior similar to a doublet near an edge. Thus, it exerts a "stronger" stopping effect and arrests the evolution of the contour close to an edge. In our calculations we have observed that this stopping behavior of the $\nabla\phi \cdot \nabla\Psi$ term allows use of large inflationary forces, resulting in features being extracted in relatively fewer time steps.

8.2 Image Feature Extraction Results

Here we sketch a few experimental results obtained using the feature extraction algorithm developed in this paper based on equation (8). First we present the result of feature extraction on a synthetic high contrast image consisting of three shapes. The image is a 150×150 binary image with intensity values 0 or 255. The entire image is used in the computations. Figure 1(a) shows the image with the initial contour. The time step used was $\Delta t = 0.000001$ and Figures 1(b) through 1(d) show the evolving contour at intermediate time steps. Figure 1(d) corresponds to 400 iterations.

In Figure 2, we present a convoluted shape to be extracted using an active contour. The image is a 150 x 150 binary image with binary intensity values as before. The entire image was used in the computations. Figure 2(a) shows the initial contour. Figures 2(b) through 2(f) show the evolving contour at 200, 400, 600, 800, and 1000 iterations. The shape of the feature has been completely captured by 1000 iterations. Again the time step used was $\Delta t = 0.000001$.

Finally, we present the result of evolution of an active contour in a real image. The aim of this experiment was to demonstrate the ability of the active contour in capturing the finer features in real images and also the abililty to capture more than one feature. The image is a 256 x 240 gray-scale image of a Rubik's cube placed on a circular table with a pattern on the table's side. An initial contour is placed with the aim of capturing the cube, the edge of the table and also the patterns on the side of the table. Figure 4(a) shows the intial contour. Figures 4(b) through 4(d) show the evolving contour after 100, 200, and 300 iterations. The time step used was $\Delta t = 0.001$. After 200 iterations the contour has captured the Rubik's cube and the table's edge. At 300 iterations most of the patterns we wished to capture on the table's side have been obtained. Indeed, the active contour finds the edge of the table from both the inside and the outside as well as the Rubik's cube itself. Notice that the snake also captures the shadow of the cube.

9 Conclusions

In this paper, we have considered a natural differential geometric approach based on image-dependent Riemannian metrics and the associated gradient flows for conformal curvature flows. This approach, applied to the segmentation problem, justifies and generalizes the

procedures of [16, 47]. Our active contours flows to the desired feature regarded as lying at the bottom of the corresponding potential energy well. Possible 3-D surface models were also proposed using these ideas. We have also considered new edge detection and segmentation schemes based on the ordinary differential equations which define geodesics relative to a given Riemannian structure. We feel that this approach is especially promising in the 3D case. We have also presented a detailed viscosity analysis and justification of our models as well as some illustrative numerical examples.

Acknowledgement: We would like to thank Professor Tryphon Georgiou of the University of Minnesota for a number of very helpful conversations.

References

[1] S. M. Allen and J. W. Cahn, "A microscopic theory for antiphase boundary motion and its application to antiphase domain coarsening," *Acta Metallurgica* **27**, pp.1085-1095, 1979.

[2] L. Alvarez, F. Guichard, P. L. Lions, and J. M. Morel, "Axiomes et equations fondamentales du traitement d'images," *C. R. Acad. Sci. Paris* **315**, pp.135-138, 1992.

[3] L. Alvarez, F. Guichard, P. L. Lions, and J. M. Morel, "Axioms and fundamental equations of image processing," Report #9216, CEREMADE, Université Paris Dauphine, 1992; *Arch. Rat. Mech. Anal.,* 1993.

[4] L. Alvarez, F. Guichard, P. L. Lions, and J. M. Morel, "Axiomatisation et nouveaux operateurs de la morphologie mathematique," *C. R. Acad. Sci. Paris,* **315**, pp. 265-268, 1992.

[5] L. Alvarez, P. L. Lions, and J. M. Morel, "Image selective smoothing and edge detection by nonlinear diffusion," *SIAM J. Numer. Anal.* **29**, pp. 845-866, 1992.

[6] L. Alvarez and J. M. Morel, "Formalization and computational aspects of image analysis," Report #0493, Department of Information and Systems, Universidad de las Palmas de Gran Canaria, 1993.

[7] B. Andrews, "Contraction of convex hypersurfaces by their affine normal," submitted for publication, 1994.

[8] S. Angenent, "On the formation of singularities in the curve shortening flow," *J. Differential Geometry* **33**, pp. 601-633, 1991.

[9] S. Angenent and M. E. Gurtin, "Multiphase thermomechanics with interfacial structure, 2: Evolution of an isothermal surface," *Arch. Rat. Mech. Anal.* **108**, pp. 323-391, 1989.

[10] S. S. Antman, "The equations for large vibrations of strings," *Amer. Math. Monthly* **87** (5), pp. 359-370, 1980.

[11] A. Blake and A. Yuille, *Active Vision*, MIT Press, Cambridge, Mass., 1992.

[12] K. A. Brakke, *The Motion of a Surface by its Mean Curvature*, "Princeton University Press, Princeton, NJ, 1978.

[13] L. Bronsard and R. V. Kohn, "Motion by mean curvature as a the singular limit of Ginzburg-Landau dynamics," *J. Diff. Eq.* **90**, pp. 211-237, 1991.

[14] L. Bronsard and F. Reitich, "On three phase boundary motion and the singular limit of a vector-valued Ginzburg-Landau equation," *Arch. Rat. Mech. Anal.* **124**, pp. 355-379, 1993.

[15] G. Caginalp, "Stefan and Hele-Shaw type models as asymptotic limits of phase field equations," *Phys. Rev. A* **39**, pp. 887-896, 1989.

[16] V. Caselles, F. Catte, T. Coll, and F. Dibos, "A geometric model for active contours in image processing," Technical Report #9210, CEREMADE, Université Paris Dauphine, 1992.

[17] V. Caselles and C. Sbert, "What is the best causal scale-space for 3D images?," Technical Report, Department of Math. and Comp. Sciences, University of Illes Balears, 07071 Palma de Mallorca, Spain, March 1994.

[18] Y.-G. Chen, Y. Giga and S. Goto, "Uniqueness and existence of viscosity solutions of generalized mean curvature flow equations," *J. Diff. Geo.* **33**, pp. 749-786, 1991.

[19] B. Chow, "Deforming convex hypersurfaces by the nth root of the Gaussian curvature," *J. Differential Geometry* **22**, pp. 117-138, 1985.

[20] M. G. Crandall and H. Ishii, "The maximum principle for semicontinuous functions," *Diff. and Integral Eqs.* **3**, pp. 1001-1014, 1990.

[21] M. G. Crandall, H. Ishii, and P.– L. Lions, "Users guide to viscosity solutions of second order partial differential equations," *Bulletin of Amer. Math. Soc.* **27**, pp. 1-67, 1992.

[22] M. P. Do Carmo, *Differential Geometry of Curves and Surfaces*, Prentice-Hall, Inc., New Jersey, 1976.

[23] M. P. Do Carmo, *Riemannian Geometry*, Prentice-Hall, Inc. New Jersey, 1992.

[24] C. L. Epstein and M. Gage, "The curve shortening flow," in *Wave Motion: Theory, Modeling, and Computation*, A. Chorin and A. Majda, Editors, Springer-Verlag, New York, 1987.

[25] L. C. Evans and J. Spruck, "Motion of level sets by mean curvature, I," *J. Diff. Geo.* **33**, pp. 635-681, 1991.

[26] L. C. Evans, H. M. Soner and P. E. Souganidis, "Phase transitions and generalized motion by mean curvature," *Comm. Pure Appl. Math.* **45**(9), pp. 1097-1123, 1992.

[27] M. Gage, "Curve shortening makes convex curves circular," *Invent. Math.* **76**, pp. 357-364, 1984.

[28] M. Gage and R. S. Hamilton, "The heat equation shrinking convex plane curves," *J. Differential Geometry* **23**, pp. 69-96, 1986.

[29] I. M. Gelfand and S. V. Fomin, *Calculus of Variations*, Prentice-Hall, Englewood Cliffs, N. J., 1963.

[30] C. Gerhardt, "Flow of nonconvex hypersurfaces into spheres," *J. Differential Geometry* **32**, pp. 299-314, 1990.

[31] M. Grayson, "A short note on the evolution of a surface by its mean curvature," *Duke Math. Journal* **58**, pp. 555-558, 1989.

[32] M. Grayson, "The heat equation shrinks embedded plane curves to round points," *J. Differential Geometry* **26**, pp. 285-314, 1987.

[33] M. Grayson, "Shortening embedded curves," *Annals of Mathematics* **129**, pp. 71-111, 1989.

[34] A. Gupta, L. von Kurowski, A. Singh, D. Geiger, C.-C. Liang, M.-Y. Chiu, L. P. Adler, M. Haacke and D. L. Wilson, "Cardiac MRI analysis: segmentation of myocardial boundaries using deformable models," preprint.

[35] M. E. Gurtin, "Toward a non-equilibrium thermodynamics of two-phase materials," *Arch. Rat. Mech. Anal.* **100**, pp. 275-312, 1988.

[36] M. Gurtin, Multiphase thermomechanics with interfacial structure, 1: Heat conduction and the capillary balance law, *Arch. Rat. Mech. Anal.,* **104** (1988) 185–221.

[37] G. Huisken, "Flow by mean curvature of convex surfaces into spheres," *J. Differential Geometry* **20**, pp. 237-266, 1984.

[38] T. Ilmanen, "Generalized flow of sets by mean curvature on a manifold," *Indiana U. Math. J.* **41**(3), pp. 671-705, 1992.

[39] M. Kass, A. Witkin, and D. Terzopoulos, "Snakes: active contour models," '*Int. Journal of Computer Vision* **1**, pp. 321-331. 1987.

[40] S. Kichenassamy, A. Kumar, P. J. Olver, A. Tannenbaum, A. Yezzi, "Gradient flows and geometric active contours," to appear in *Proceedings of the Fifth International Conference on Computer Vision.*

[41] B. B. Kimia, A. Tannenbaum, and S. W. Zucker, "Toward a computational theory of shape: An overview", *Lecture Notes in Computer Science* **427**, pp. 402-407, Springer-Verlag, New York, 1990.

[42] B. B. Kimia, A. Tannenbaum, and S. W. Zucker, "Shapes, shocks, and deformations, I," to appear in *Int. J. Computer Vision.*

[43] B. B. Kimia, A. Tannenbaum, and S. W. Zucker, "On the evolution of curves via a function of curvature, I: the classical case," *J. of Math. Analysis and Applications* **163**, pp. 438-458, 1992.

[44] A. Kumar, *Visual Information in a Feedback Loop*, Ph. D. thesis, University of Minnesota, 1995.

[45] R. J. LeVeque, *Numerical Methods for Conservation Laws*, Birkhäuser, Boston, 1992.

[46] P. L. Lions, *Generalized Solutions of Hamilton-Jacobi Equations*, Pitman Publishing, Boston, 1982.

[47] R. Malladi, J. Sethian, and B. Vemuri, "Shape modeling with front propagation: a level set approach," *IEEE Trans. Pattern Anal. Machine Intell.* **17**, pp. 158-175, 1995.

[48] F. Mokhatarian and A. Mackworth, "A theory of multiscale, curvature-based shape representation for planar curves," *IEEE Trans. Pattern Anal. Machine Intell.* **14**, pp. 789-805, 1992.

[49] F. Morgan, *Riemannian Geometry*, John and Bartlett Publishers, Boston, 1993.

[50] P. de Mottoni and M. Schatzman, "Evolution géométrique d'interfaces," *C. R. Acad. Sci. Paris, sér. I Math.* **309**, pp. 453-458, 1989.

[51] W. W. Mullins, "Theory of thermal grooving," *J. Appl. Phys.* **28**, pp. 333-339, 1957.

[52] P. Neskovic and B. Kimia, "Three-dimensional shape representation from curvature-dependent deformations," Technical Report #128, LEMS, Brown University, 1994.

[53] R. H. Nochetto, M. Paolini, and C. Verdi "A dynamic mesh method algorithm for curvature dependent evolving interfaces," Technical Report, University of Maryland, 1994.

[54] P. J. Olver, G. Sapiro, and A. Tannenbaum, "Geometric invariant evolution of surfaces and volumetric smoothing," to appear in *SIAM J. Math. Anal.*, 1994.

[55] S. Osher, "Riemann solvers, the entropy condition, and difference approximations," *SIAM J. Numer. Anal.* **21**, pp. 217-235, 1984.

[56] S. J. Osher and J. A. Sethian, "Fronts propagation with curvature dependent speed: Algorithms based on Hamilton-Jacobi formulations," *Journal of Computational Physics* **79**, pp. 12-49, 1988.

[57] S. Osher and L. I. Rudin, "Feature-oriented image enhancement using shock filters," *SIAM J. Numer. Anal.* **27**, pp. 919-940, 1990.

[58] P. Perona and J. Malik, "Scale-space and edge detection using anisotropic diffusion," *IEEE Trans. Pattern Anal. Machine Intell.* **12**, pp. 629-639, 1990.

[59] M. H. Protter and H. F. Weinberger, *Maximum Principles in Differential Equations,* Springer-Verlag, New York, 1984.

[60] J. Rubinstein, P. Sternberg and J. B. Keller, "Fast reaction, slow diffusion, and curve shortening," *SIAM J. Appl. Math.* **49**(1), pp. 116-133, 1989.

[61] G. Sapiro and A. Tannenbaum, "Affine invariant scale-space," *International Journal of Computer Vision* **11**, pp. 25-44, 1993.

[62] G. Sapiro and A. Tannenbaum, "On invariant curve evolution and image analysis," *Indiana Univ. Journal of Math.* **42**, 1993.

[63] J. A. Sethian, *An Analysis of Flame Propagation*, Ph. D. Dissertation, University of California, 1982.

[64] J. A. Sethian, "Curvature and the evolution of fronts," *Commun. Math. Phys.* **101**, pp. 487-499, 1985

[65] J. A. Sethian, "A review of recent numerical algorithms for hypersurfaces moving with curvature dependent speed," *J. Differential Geometry* **31**, pp. 131-161, 1989.

[66] J. A. Sethian and J. Strain, "Crystal growth and dendritic solidification," *Journal of Computational Physics* **98**, 1992.

[67] J. Smoller, *Shock Waves and Reaction-diffusion Equations*, Springer-Verlag, New York, 1983.

[68] G. A. Sod, *Numerical Methods in Fluid Dynamics*, Cambridge University Press, Cambridge, 1985

[69] M. Spivak, *A Comprehensive Introduction to Differential Geometry*, Publish or Perish Inc, Berkeley, California, 1979.

[70] H. Tek and B. Kimia, "Deformable bubbles in the reaction-diffusion space," Technical Report #138, LEMS, Brown University, 1994.

[71] D. Terzopoulos and A. Witkin, "Constraints on deformable models: recovering shape and non-rigid motion," Artificial Intelligence **36**, pp. 91-123, 1988.

[72] D. Terzopoulos and R. Szelski, "Tracking with Kalman snakes," in *Active Vision* edited by A. Blake and A. Zisserman, MIT Press, Cambridge, Mass., 1992.

[73] B. White, "Some recent developments in differential geometry," *Mathematical Intelligencer* **11**, pp. 41-47, 1989.

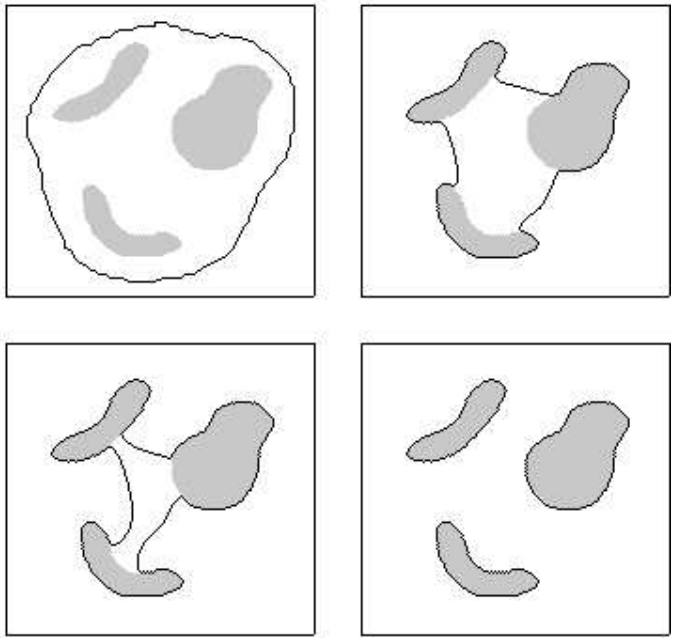

Figure 1: Feature extraction in a synthetic image. Left to right, top to bottom: (a) Initial contour. (b),(c),and (d) contour after 200, 300, and 400 iterations. $\Delta t = 0.000001$.

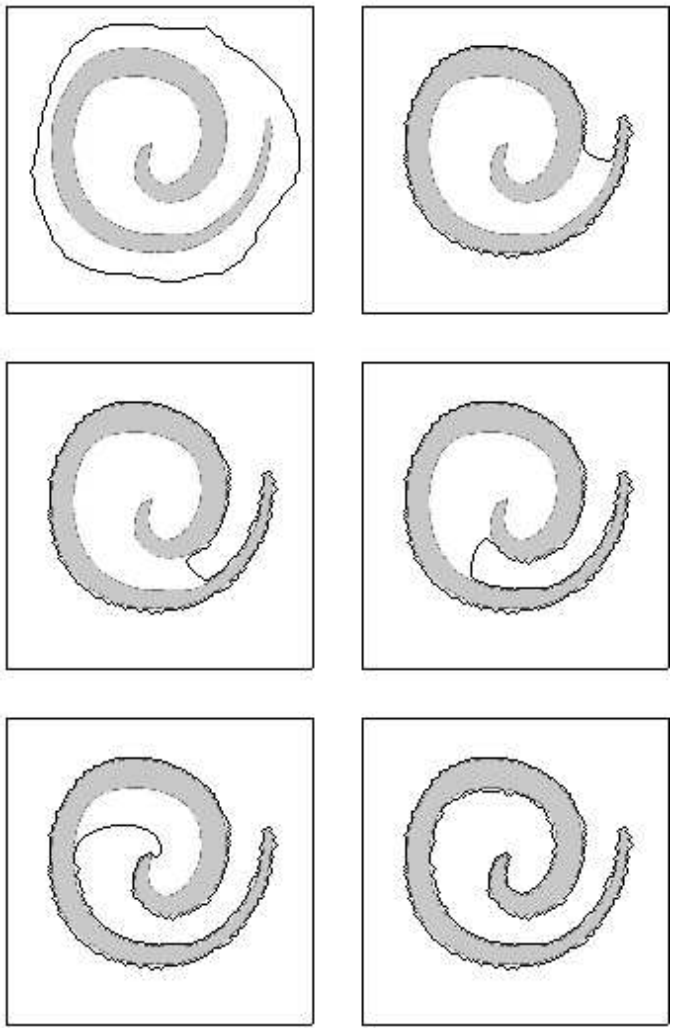

Figure 2: Feature extraction in a synthetic image. Left to right, top to bottom: (a) Initial contour. (b),(c),(d),(e),and (f) contour after 200, 400, 600, 800 and 1000 iterations. $\Delta t = 0.000001$.

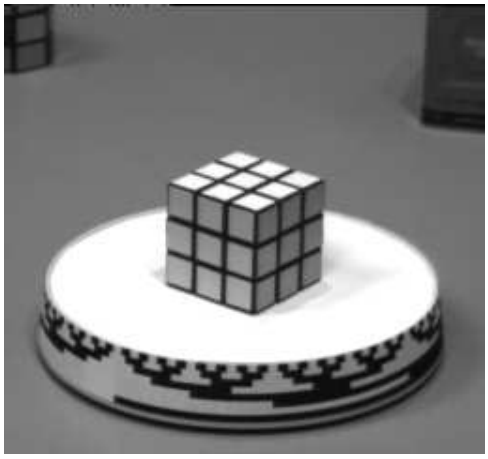

Figure 3: Rubik's Cube on a turntable.

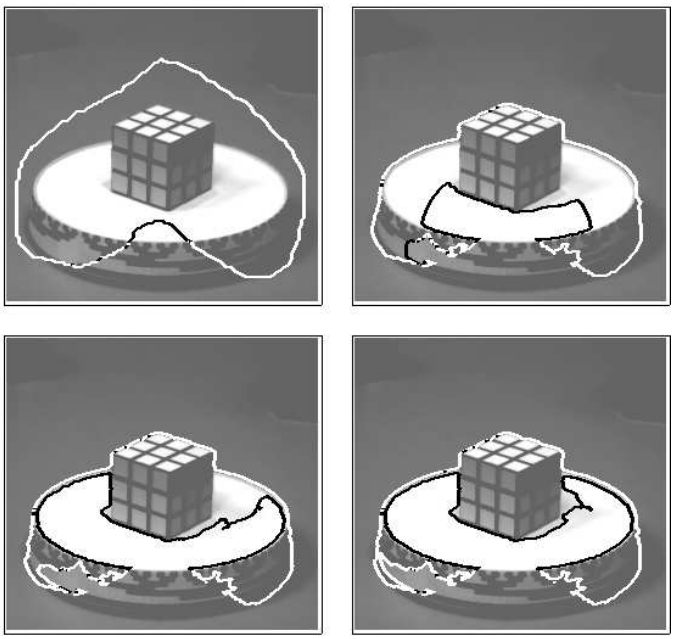

Figure 4: Feature extraction in a real image. Left to right, top to bottom: (a) Initial contour. (b),(c),and (d) contour after 100, 200, and 300 iterations. $\Delta t = 0.001$.